Desalination and Water Treatment
www.deswater.com

doi: 10.5004/dwt.2022.28800

271 (2022) 244–253
September

Synthesis of recyclable magnetic attapulgite for purifying oily wastewater

Haitao Liang, Yonghong Wu*, Fei Wang, Bing Zhang*

School of Petrochemical Engineering, Shenyang University of Technology, Liaoyang 111003, China, emails: wuyh@sut.edu.cn (Y. Wu), bzhangdut@163.com/zhangbing@sut.edu.cn (B. Zhang), 252654500@qq.com (H. Liang), feiwang301@163.com (F. Wang)

Received 14 January 2022; Accepted 5 August 2022

ABSTRACT

Magnetically functionalized attapulgite (ATP) was synthesized by loading Fe_3O_4 onto ATP via co-precipitation method. The surface functional groups, thermal stability, microstructure, morphology, and magnetic properties of the samples were measured by Fourier-transform infrared spectroscopy, thermogravimetric analysis, X-ray diffraction, scanning electron microscope and vibrating magnetometer, respectively. The oil removal and recovery of magnetic ATP for oil-in-water emulsion was investigated. The results show that the magnetic ATP exhibits a saturation magnetization M_s of 1.5 emu/g, the coercivity H_c of 10 Oe and the residual magnetization M_r of 0.03 emu/g. In addition, the thermal stability and the dispersibility in oil-water emulsion of ATP is significantly improved by Fe_3O_4 modification. The adsorption capacity of ATP for emulsified oil slightly decreases from 8.14 to 7.16 mg/g after Fe_3O_4 modification, regardless of the effect of acid treatment or increment of loading amount. In particular, the modified ATP is easily recovered by an external magnetic field.

Keywords: Adsorption; Emulsion; Environmental protection; Magnetic functionalization; Oil removal

1. Introduction

Oily wastewater is widely by-produced from almost all sections of mankind's daily life, industrial production, as well as some unexpected accidents [1]. The random discharge of oily wastewater will certainly cause serious pollution to the water bodies, deterioration to climate change and the huge threat to human health [2]. Therefore, great effort has been paid for the treatment of oily wastewater. Overall, the treatment technologies of oily wastewater mainly include physical method, chemical method and biological method [3]. Chemical method is frequently restricted by the disadvantages of large dosage of chemical addition and risk of secondary pollution to environment [4,5]. Besides, biological method is commonly suffered by the drawbacks of high capital for investment and maintenance, complex construction and tedious sludge cleaning [6]. In contrast, physical method, for example, adsorption, is more easy implementation, low cost and high efficiency for treating oily wastewater, although it usually exhibits inferior selectivity and short service life [3]. Adsorption mainly relies on the preferential adsorption of adsorbents towards specific adsorbates in the solution through physical or chemical interactions so as to separate them from the solution [7]. Therefore, the structural characteristics and surface properties of adsorbents play a crucial role in the determination of separation efficiency and economical competition of adsorption technology [8]. As such, the development of efficient adsorbents is an everlasting key issue of adsorption technology.

Attapulgite (ATP) is an excellent natural mineral soil with extremely abundant reserves in nature and greatly promising prospects for applications [9–11]. ATP is widely used as carriers of industrial catalyst, adsorbents of heavy metal particles, decolorant of colored liquids, as well as the remedy agent of environmental pollution and

* Corresponding authors.

wastewater treatment, etc. [11–13]. As an adsorbent, ATP is frequently suffered from the issues of recovery and recycle in practice especially for fine particles [14]. As a matter of fact, fine particles are more favorable for the removal efficiency of pollutants due to the increased specific area and reduced intrapaticulate transport resistance [15]. Unfortunately, it would be more difficult for recycling the spent ATP from water or even resulting into secondary pollution in application as the result of diminishing particle size [16].

In order to overcome this issue, magnetically functional adsorbents have gained much interest in recent years [17,18]. By this means, it could easily control the distribution of adsorbents during adsorption and conveniently recovery them from aqueous solution by external magnetic force, and thereby increases the separation efficiency, added-value and performance-cost ratios of adsorbents [19].

Generally speaking, magnetic adsorbents can be produced by solvothermal method, co-precipitation method, physical transformation method, etc. [20]. Among them, the co-precipitation method is more promising owing to the simple route, short time, low cost, and mild reaction conditions during preparation [21]. Liu et al. [22] prepared attapulgite/Fe_3O_4 magnetic nanomaterials by co-precipitation technique, which was proposed to be potential for the magnetic fluid and the biological medicine field. Deng et al. [23] synthesized magnetic ATP with an excellent magnetism for propranol removal. Wang et al. [20] prepared a novel environmental-friendly nanocomposite magnetic ATP functionalized by chitosan and EDTA for cadmium(II) removal, with the maximum cadmium adsorption capacity of 127.79 mg/g. Niu et al. [24] modified ATP by magnetic metal–organic frameworks for magnetic solid phase extraction and determinations of benzoylurea insecticides in tea infusions, with a rapid and efficient extraction as well as good recycling stability. Ji et al. [25] eliminated aflatoxin B_1 from contaminated peanut oils with an optimum removal of 86.82% using magnetic ATP made by impregnation precipitation method. All in all, the documents have demonstrated that magnetic ATP adsorbents have shown quite feasible and promising prospect for the removal of various pollutants in wastewater by adsorption. Nevertheless, no work has conducted for the treatment of oily wastewater with magnetic ATP so far to the best of our knowledge.

Here, an attempt was made for the first time to treat oil-water emulsion by magnetic ATP synthesized by chemical co-precipitation method. Moreover, the possible adsorption behavior of oils onto the as-prepared magnetic ATP was roughly investigated with respect to thermodynamics and kinetics. We are sure that the present work would lay a theoretical and practical foundation for promising applications of functionalized ATP adsorbents in related fields.

2. Experimental

2.1. Raw materials

The main raw materials used are: ATP powder (average particle size of 7.0 μm) produced from Jiangsu Yitai (China), $FeCl_3 \cdot 6H_2O$ (AR) from Tianjin Runjinte Chemical Co., Ltd., (China), $FeSO_4 \cdot 7H_2O$ (AR) from Tianjin Bodi Chemical Co., Ltd., (China), ammonia water $NH_3 \cdot H_2O$ (GR) from Sinopharm Group Chemical Reagent Co., Ltd., (China), hydrochloric acid (GR) and absolute ethanol (AR) from Tianjin Fuyu Fine Chemical Co., Ltd., (China). In addition, the crude oil from Russia Turmin oil field was offered by PetroChina Liaoyang Petrochemical Company.

2.2. Preparation of magnetic ATP

Here, classical co-precipitation method was used to prepare magnetic ATP [22,26]. First of all, 8.34 g of ATP was put into a bottle of 200 mL HCl with 5 wt.% concentration and then kept stirring for 2 h. After setting down and skimming off the supernatant, the remaining sample was repeatedly washed with distilled water until to neutrality. Then, a solid product of acid-purified ATP was obtained by filtration of the liquid phase. Subsequently, the product was dried at 100°C for 2 h and screened by a 100-mesh sieve (<150 μm) for use.

After that, 2 g ATP was dispersed into a beaker containing 50 mL absolute ethanol to form a suspension. Then, 0.47 g or 0.7 g $FeCl_3$ was dissolved into the above suspension, followed by ultrasonic dispersion for 30 min. At the same time, 0.47 g or 0.7 g $FeSO_4$ was dissolved in another 5 mL distilled water to obtain Fe^{2+} solution. The latter solution was quickly mixed into the former ATP-$FeCl_3$ suspension. Furthermore, $NH_3 \cdot H_2O$ was slowly dropped into the suspension under vigorously stirring till to the solution turns dark green. At this moment, the solution was quickly transferred to a 90°C water bath and allowed for natural crystallization for 1 h. Finally, the solid samples were washed alternately with distilled water and absolute ethanol to neutrality, and then dried at 60°C to remove remaining moisture.

For convenience, the samples were marked with H-ATP/Fe_3O_4(x), referring to the acid-treated ATP with loading x% of Fe_3O_4. Where, x means the magnetic loading amount (20 and 30 wt.%).

2.3. Application for oily wastewater treatment

2.3.1. Configuration of oil-water emulsion

A tiny amount of crude oil was dropped into a beaker containing double-distilled water. Then, uniform emulsion was formed by fully smashing the crude oil into tiny suspended droplets with ultrasonic dispersion. Finally, it was diluted to a 100 mg/L solution. The oil-water mixture by such processes could remain steady at an average droplet size of ca.535 μm for several days, presenting a typical characteristic of oil-in-water emulsion [27].

2.3.2. Determination of oil removal by adsorption

The experiment was conducted by taking 1.0 g ATP as adsorbent in an Erlenmeyer flask containing 100 mL oil-water emulsion. The flask was kept shaking at 30°C for 1 h in a constant-temperature water bath shaker (SHA-C type, Changzhou Guohua Electric Co., Ltd., China). After adsorption, the spent ATP was easily aggregated and recovered from the solution with the help of an external magnetic field.

According to the concentrations of the solution before and after adsorption, the adsorption capacity for oils was calculated by Eq. (1). Here, the concentration was measured by a UV-visible spectrophotometer (model UV-1800.PC).

$$M_a = \frac{\left(C_f - C_a\right) \times 100\text{mL}}{1.00g \times 1000} \quad (1)$$

Besides, the oil removal percent (R) was estimated using Eq. (2).

$$R = \left[\frac{C_f - C_a}{C_f}\right] \times 100\% \quad (2)$$

where M_a the adsorption capacity (mg/g), R the oil removal percent (%), C_f and C_a the emulsified oil concentration of oily wastewater before and after adsorption (mg/L), respectively.

2.4. Sample characterization

The morphology of the samples was observed by scanning electron microscope (SEM, JEM-7500F cold field-emission SEM, JEOL Company) and transmission electron microscope (TEM, JEM-2100 by JEOL Company).

The thermal stability of the samples was measured by a thermogravimetric analyzer (TGA, TGA 4000, PerkinElmer, USA).

The microstructure of the samples was detected by an X-ray powder diffractometer (XRD, X'Pert Pro MPD type, PHILIPS, Netherlands).

The functional groups on the sample surface were inspected by a Fourier-transform infrared spectrometer (FTIR, TENSOR II type, Bruker, Germany).

The magnetic property of the magnetic compositions was detected by a 7400 vibrating sample magnetic (VSM) intensity analyzer (Shanghai Yihong Scientific Instrument Co., Ltd.) through the induced electron potential that was produced in the built-in coil of the instrument by repeatedly and rapidly vibrating the sample in a magnetic field.

3. Results and discussion

3.1. Structure and property analysis

3.1.1. Surface functional groups

Fig. 1 shows the FTIR spectra. In the original ATP spectrum, the characteristic absorption peaks can be clearly seen for carbonate impurities at 1,420, 875, and 730 cm^{-1}, and the stretching vibration of Si–O bond in the SiO_2 framework at 1,080 cm^{-1}, the bending vibration of –OH in the aluminum-oxygen octahedron at 827 cm^{-1}, the vibration of silicon-oxygen structure at 563 cm^{-1}, and the characteristic peak of O–Si–O bond at 465 cm^{-1} [20]. After acid treatment, the peaks for carbonate impurity at 1,420 and 875 cm^{-1} disappear, indicating that those species have been successfully eroded [28]. At the same time, the vibration peaks of surface silicon-oxygen stretching and the bending vibration peak of hydroxyl in the aluminum oxide octahedron are enhanced because more of the main skeleton structure is exposed on the surface of ATP.

By contrast, the spectrum profile of the magnetized ATP is almost identical to the original ATP. However, the peak intensity of Fe–O for the former is reduced due to the overlap of the Fe–O bond characteristic peaks (540, 558, and 555 cm^{-1}) in Fe_3O_4 with the bending vibration peak of Si–O–Si (563 cm^{-1}) in ATP.

In addition, compared with acid-modified ATP, the characteristic peaks of magnetized ATP are enhanced at 1,080, 827, 551, and 449 cm^{-1}, while the position for the latter slightly shifts at 449 cm^{-1}. The reason is that the overlapping of vibration peak of Fe–O (539 cm^{-1}) in magnetized ATP with the typical absorption peaks of ATP. It confirms the successful loading of Fe_3O_4 in the magnetized ATP.

3.1.2. Morphology observation

Fig. 2 shows the SEM and TEM images of ATP. The original ATP has a number of irregular lumpy particles, that is, dense agglomerated impurities of carbonate crystals and calcium oxide on the surface and inside of ATP. The crystal impurities are tightly wrapped on the surface appearance of ATP, resulting into the resistance of exposing active ingredients towards surrounding medium [20]. After acid treatment, a part of ATP with rod-like morphology is disclosed although most of them are still in flake shape on the whole. It suggests that a portion of impurities has been eliminated [29]. This is consistent with the above FTIR analysis.

In contrast, more finely granular deposits can be found on the surface of magnetized ATP. It is identified as Fe_3O_4 grains with a particle size of less than 50 nm from the locally magnified images, which are derived from the hydrolysis and crystallization on the surface of ATP [20]. These magnetic particles are uniformly deposited on the surface of ATP, which will definitely affect the pore structure, surface morphology and adsorption properties.

Besides, the TEM images also confirm that a large amount of amorphous salts present on the surface of the original ATP. After acid washing, some regular microstructural morphological structures are uncovered, especially the presence of a large amount of Fe_3O_4 features for magneticalized ATP.

3.1.3. Microstructure analysis

As shown in Fig. 3, the diffraction peaks in XRD patterns of ATP can be assigned as the typically microstructural reflections for (200), (310), (400), (102), and (600) planes at 2θ = 13.7°, 21.5°, 27.5°, 34.5°, and 42.5°, respectively [19]. Judging by the weak peak intensities of ATP and H-ATP, the crystallinity of the original ATP is quite low. In particular, many of the above-mentioned diffraction peaks of original ATP are concealed by a large amount of impurities, for example, carbonates [25]. As a consequence, the effective framework of original ATP does not work completely. After acid purification, some local ATP skeleton is exposed due to the impurities removal. This is consistent with the results discussed earlier.

For ATP loaded with Fe_3O_4, most of the characteristic diffraction peaks of ATP are reduced due to the masking

effect of Fe_3O_4. This can be confirmed by the presence of the typical diffraction peak of Fe_3O_4 in the patterns. In summary, the microstructure analysis has shown that Fe_3O_4 magnetically functionalized ATP was successfully prepared.

3.1.4. Thermal stability analysis

Fig. 4 shows the thermal weight loss of samples in the pyrolysis temperature range of 100°C–800°C. For original ATP, the weight loss successively increases to 6% in the temperature range of 100°C–600°C, due to the removal of adsorbed water and crystal water in ATP [30]. In addition, another weight loss of 4% between 600°C–800°C is attributed to the decomposition of impurities such as carbonate in ATP. Despite acid treatment, the profile of weight loss curve of H-ATP does not change obviously compared with the pristine one, but the weight loss is significantly reduced in magnitude by nearly 50%. It means that the impurities of the original ATP contribute more than half of the overall weight loss.

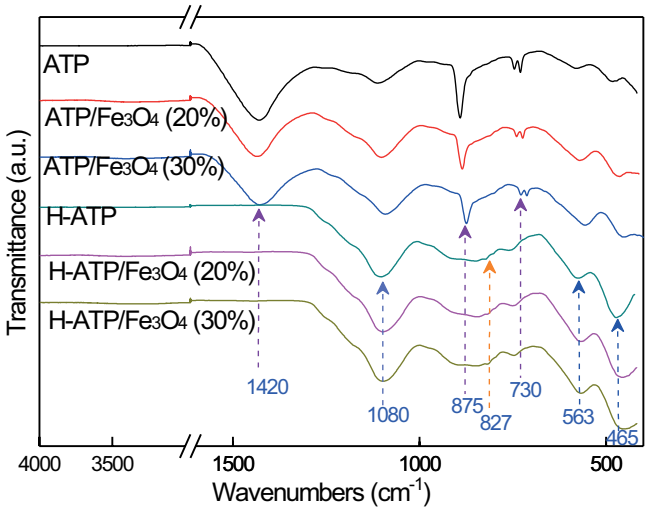

Fig. 1. FTIR spectra of samples.

Interestingly, the weight loss curves of ATP/Fe_3O_4 and the original ATP are intercrossed at 650°C. This suggests that the pyrolysis behavior of ATP has affected by the incorporation of Fe_3O_4. In actual, some impurities in ATP react with Fe_3O_4 before 650°C, along with the release of reduced gases (e.g., CO_2, etc.) and production of ferrous oxide or iron element, resulting into some weight loss. Differently, the overall thermal stability is rather stable when ATP is loaded with more Fe_3O_4 (20%–30%). Therefore, the weight loss remains nearly unchanged after 650°C. Similarly, the comparison of H-ATP and H-ATP/Fe_3O_4 samples proves that loading Fe_3O_4 significantly enhances the thermal stability of ATP.

In addition, the spent ATP/Fe_3O_4 is more thermally stable than the pristine ATP before 650°C. Oppositely, the thermal degradation curve of the former drops rapidly as the temperature further increases. Above 720°C, the weight loss of spent ATP/Fe_3O_4 becomes lower than the pristine one. This change tendency continues to keep decreasing sharply until to the final pyrolysis temperature of 800°C. The reason is that the oil layer deposited on the surface of the adsorbent transforms into a dense carbon

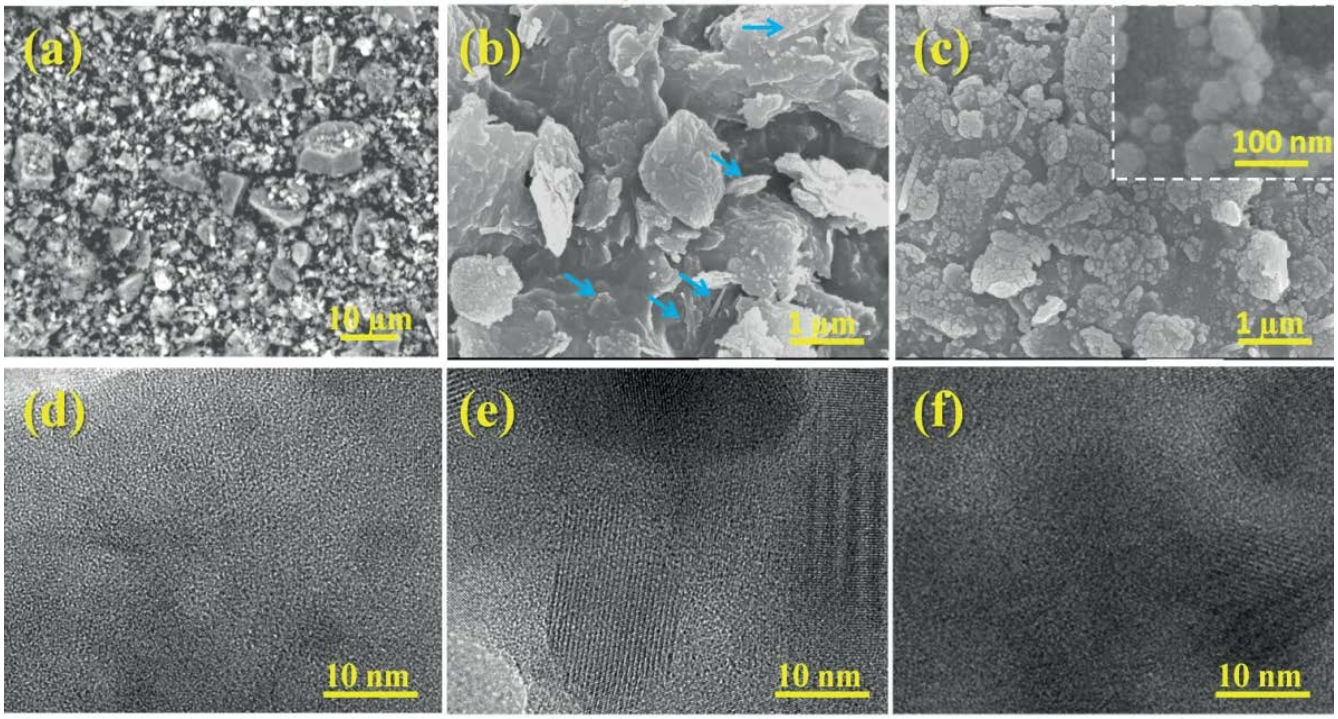

Fig. 2. Electron micrographs of the samples. SEM: (a) original ATP, (b) HCl-ATP, (c) H-ATP/Fe_3O_4; TEM: (d) original ATP, (e) HCl-ATP, (f) H-ATP/Fe_3O_4.

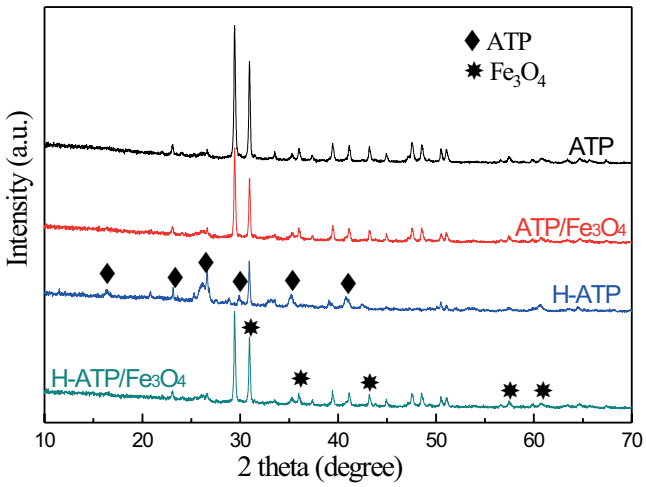

Fig. 3. XRD patterns of ATP samples.

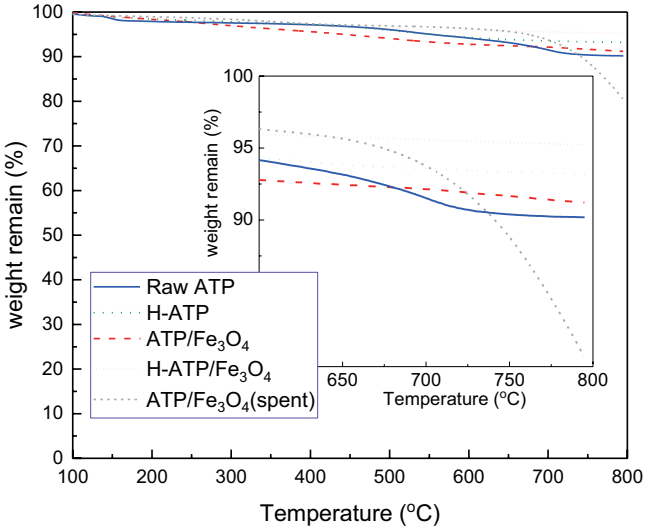

Fig. 4. Thermal weight loss curve of ATP sample.

layer under low pyrolysis temperature, which retards the thermal decomposition of impurities in ATP and the reduction reaction of Fe_3O_4. Meanwhile, the thermal decomposition reaction occurs rapidly with a large weight loss when the temperature further increases above 650°C due to the rupture of surface carbon layer as the result of particle expanding and the quick occurrence of thermal degradation.

3.1.5. Magnetic performance analysis

Fig. 5 shows the VSM hysteresis loop of the sample ATP/Fe_3O_4. The as-prepared magnetic ATP exhibits quite well ferromagnetism. The hysteresis loop is an S-shaped curve. Namely, the magnetic properties of ATP/Fe_3O_4 gradually increase and finally reach equilibrium as the intensity of the applied external magnetic field increases. At the same time, the intensity of ATP/Fe_3O_4 also reaches to another equilibrium state when the reverse magnetic field is applied. According

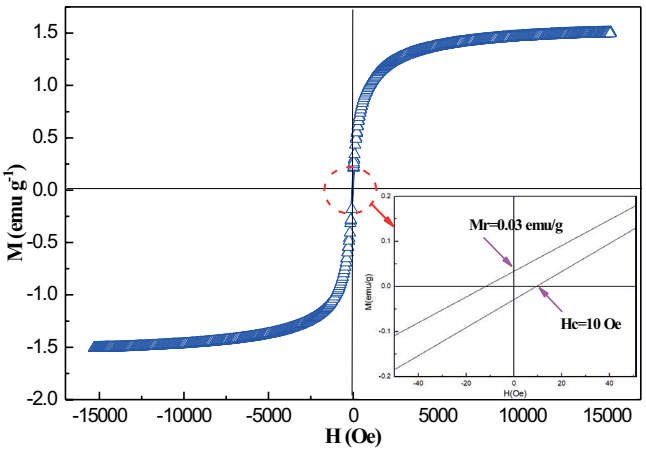

Fig. 5. Magnetic attapulgite VSM hysteresis loop.

to the calculation results, the values of hysteresis parameters are coercivity H_c = 10 Oe, remanent M_r = 0.03 emu/g, magnetization M_s = 1.5 emu/g, respectively. Those values are comparable to the data in literature [19].

As a matter of fact, the coercivity of the synthesized magnetic ATP is a bit of little, which is in accordance to the paramagnetic characteristics. It is ascribed to the small particle size of the ferroferric oxide crystal on the surface of ATP. In summary, the above result has verified that the ATP is typical ferrimagnetism belonging to a standard soft magnetic material, which is consistent with the magnetic properties of small particle size ferroferric oxide [20]. For such magnetic materials, the inside magnetons will be arranged in anti-parallel with the net magnetization of none zero if no external magnetic field is applied. Therefore, the outstanding magnetic property of ATP can ensure the effective recovery from water by external magnetic field.

3.2. Separation of oil-water emulsion

3.2.1. Adsorption results

Fig. 6 shows the adsorption capacity and removal rate of emulsified oil for the as-produced ATP samples. The adsorption amount and removal rate of ATP/Fe_3O_4 composites are somewhat inferior to those of the original ATP. For example, the adsorption capacity decreases from 8.14 mg/g of original ATP to 7.16 mg/g of ATP/Fe_3O_4 (20%), together with the reduction of oil removal rate from 81.37% to 71.57%. Moreover, the decreasing trend is steeper with increasing the loading amount of Fe_3O_4. In particular, the acid treated ATP is greatly reduced by four times. This result is in good agreement with reports on ATP modified with magnetic materials for adsorption of other systems [13]. The decrease in adsorption capacity is related to the adsorption mechanism of modified ATP. It is speculated that the present ATP mainly relies on the physical adsorption closely related to the specific surface area. Wang et al. [31] found that the specific surface area decreased from 137 to 114 m^2/g when ATP was loaded with MgO. Likewise, loading Fe_3O_4 certainly reduces the specific surface area and the amount of adsorption active sites of ATP. Therefore, it is suggested that future research direction

on the surface modification of such adsorbents should be devoted to the introduction of magnetically functional groups, ion exchange, electrostatic attraction or chelation, to remove pollutants [16].

Anyhow, the oil removal performance of present functionalized ATP is comparable to that of reports as shown in Table 1 [32–40]. Although their benchmarks are largely different, the results may also insight into the potential use of the as-prepared ATP in the field of oily wastewater treatment, in addition to the easy recovery properties as will be discussed in the later section of this work.

Apart from the structure and properties of the adsorbent itself, the adsorption efficiency is also tightly associated with the operation factors such as the adsorbent dosage, contact time, adsorption temperature, pH value, etc. [41,42]. Usually, the adsorbate removal would be increased with elevating the adsorbent dosage due to the improvement of accessible adsorption sites. Oppositely, the adsorption capacity of adsorbents might be reduced if the adsorbent dosage is extremely high owing to the particulate overlapping and aggregation that tends to diminish the effective adsorption sites in a given volume [43]. Therefore, the adoption of optimum adsorbent dosage is favorable not only for improving the adsorption efficiency but also for minimizing the operation cost. In contrast to dosage, the control of contact time is easier except for reserving sufficient span time for approaching adsorption saturation of adsorbents during batch experiments. In case of temperature, it is most likely to increase the diffusion rate of adsorbates and easily achieve the equilibrium state at higher temperature. However, the negative aspect is promoting desorption of adsorbates from adsorbents at the same time. Consequently, in order to reach a higher adsorption capacity, it is suggested to conduct adsorption at lower temperature and prolonger time [44]. Besides, pH values of solution might also take effects on the surface properties and binding sites of the adsorbent so as to influence the oil removal. In common, the oil droplets in emulsions are negatively charged, therefore, the stability of emulsions can be reduced and aggregation promoted by charge neutralization. It was found that a decrease in pH can reduce the zeta potential, which affects the stability of emulsions, thus leading to breakage and thus formation of larger oil droplets and improving the adsorption of oil by adsorbent materials [45]. On the contrary, alkaline conditions might be capable of saponification reactions that lead to hydrolysis of the oil, while acidic conditions can open some pores that are blocked by adsorbents, which in turn improve the adsorption capacity and facilitate the adsorption of the oil [46]. Amazingly, there are some adsorbents that have no effect on the change of pH value [47]. In the treatment of oily wastewater, the adsorption material that does not require pH adjustment to achieve a good adsorption effect should be selected as much as possible. This is favorable for both simplifying the treatment process of oily wastewater and reducing the treatment cost.

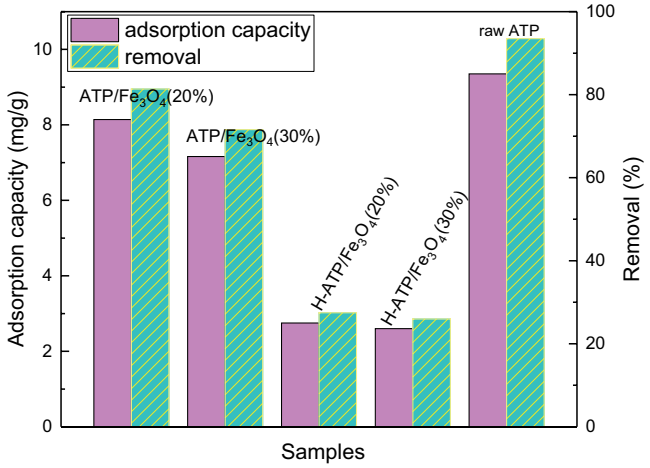

Fig. 6. Adsorption of ATP samples to emulsified oil.

Among the various operating parameters, statistical methods are applicable for variance analysis in order to rank their sequence [48,49]. For instance, Ahmadpour et al. [50] found that the factors followed the order of catalyst dose > DCF concentration > pH > aeration and magnetic stirrer during the study of photocatalytic degradation of pharmaceutical pollutant by applying a statistical analysis methodology.

In short, the selection of the adsorption conditions used in this work was based on the properties and performance of some similar adsorbents in reports [32,34,37,39]. Nevertheless, in order to fully understand the relevant

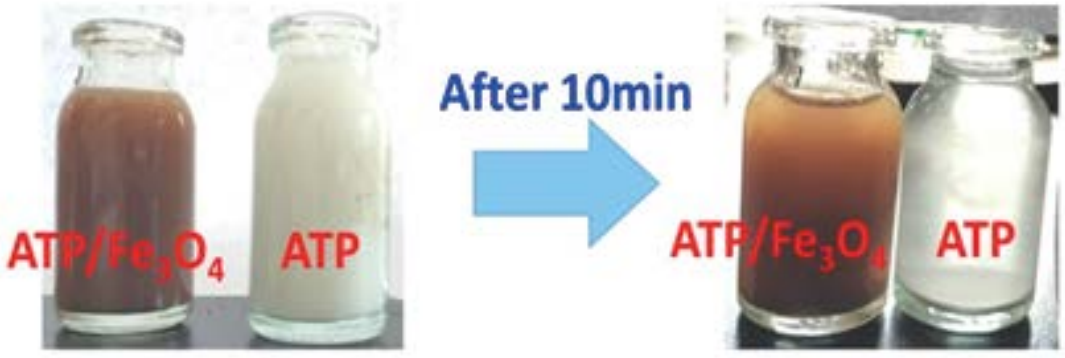

Fig. 7. Deposition of adsorbents in oil-water emulsion.

adsorption mechanism, further in-depth and systematic experimental studies are needed in the future.

The photos in Fig. 7 have shown that the present ATP/Fe_3O_4 is well remained a suspension state for a long time because of the excellent dispersibility in oil-water emulsion compared with original ATP. On the contrary, the pristine ATP has quickly settled down to the bottom of the emulsion after 10 min.

Anyhow, it needs certain time for spent ATP to regenerate its adsorption performance. Thus, it is of more practical significance if the ATP is made into a filter membrane material. At present, our research group is carrying out the related work.

3.2.2. Adsorbent recovery

As shown in Fig. 8, the dark brown fine particles of magnetic ATP adsorbed by the oil droplets obviously aggregate together on the magnet when the neodymium-iron-boron strong magnet is put into the emulsion. As such, it makes the recovery of ATP more efficient and rapid. After 5 min, the solution becomes clear and transparent, indicating that the adsorbent and the liquid solution are completely separated with quite well recovery efficiency [51]. Differently, the pure ATP can only be separated from the liquid by natural sedimentation or centrifugal separation with more tedious equipment and operations, let alone the incomplete recovery of the spent ATP from solution [13].

3.2.3. Theoretical analysis

Generally, there are three most popular isotherm models to depict the adsorption behaviors, that is, Langmuir, Freundlich and Temkin [51]. As shown in Table 2, most oil-water adsorption systems obey the isotherm models of Langmuir and Freundlich, but Temkin [32,36,37,46,47]. It suggests that the process of oil adsorption on solid adsorbents is mainly governed by the monolayer adsorption on the homogeneous surface or multilayer adsorption on the heterogonous surface by physisorption rather than chemisorption [52].

The study of adsorption kinetics is mainly used to describe the adsorption rate of the adsorbent on the solute and determine the control mechanism of the surface adsorption process [51]. The adsorption mechanism could be further discussed by fitting the data with the kinetic models. In Table 2, it shows that most oil-water adsorption systems are fitted well with the pseudo-second-order kinetic model [17].

In a common sense, the adsorption of present solid ATP/Fe_3O_4 can be divided into external surface adsorption and internal surface adsorption. Since the pore size of

Table 1
Comparative result of different adsorbents for oil adsorption

No.	Adsorbents	Oil type	Sorbent dose, g/L	Oil concentration, g/L	Adsorption capacity	Removal, %	References
1	Algal biomass	Crude oil	10	10	–	72	[32]
2	Hydrogel	Toluene, rapeseed oil, olive oil, engine oil, hexadecane	as filter	9.95 wt.%	–	>98	[33]
3	Graphene sponge	Toluene	–	1%–10%	6.5 g/g	60–80	[34]
4	Hafnium oxide (MHO) ceramic	Crude oil	–	3 g/L	–	99.9	[35]
5	Fe_3O_4/chitosan	Diesel	0.456	–	157.74 mg/g	–	[36]
6	Bentonite	Oilfield samples	1	1.012	–	98.32	[37]
7	PAC	Oilfield samples	1	0.836	–	93.54	[37]
8	Cellulose aerogel	Diesel	–	–	5.85 mg/g	–	[38]
9	Graphene aerogel	Crude oil	–	–	60–110 g/g	–	[39]
10	Graphene aerogel	Diesel	–	–	2.5×10^4 mg/g	–	[40]
11	ATP/Fe_3O_4	Crude oil	1.0	100 mg/L	7.16 mg/g	71.57	This work

Table 2
Kinetic and isotherm models for oil-water adsorption systems in reports

No.	Adsorbents	Oil types	Kinetic models	Isotherm models	References
1	Chitosan	Residue oil from palm oil mill effluent	Pseudo-second-order	Freundlich	[46]
2	Algal biomass	Crude oil	Pseudo-second-order	Langmuir	[32]
3	Resins XAD 7 and L 493	Gasoline	Pseudo-second-order	Langmuir	[47]
4	Fe_3O_4/chitosan	Diesel	Pseudo-second-order	Langmuir	[36]
5	Bentonite, PAC	Oilfield samples	–	Freundlich	[37]

Fig. 8. Recovery efficiency of magnetic ATP from oil-water solution by strong magnetic field.

ATP is about 0.38 nm × 0.63 nm, the diameter of ions and molecules must be smaller than the pore size of ATP/Fe_3O_4 in order to complete the internal surface adsorption [23]. Namely, the larger molecules cannot be adsorbed by the internal surface of the ATP/Fe_3O_4 except for the outer surface. Therefore, the adsorption of ATP/Fe_3O_4 in wastewater treatment is mainly ascribed to the external surface adsorption [24]. Because of the structural and surface charges, the adsorption on the external surface of ATP/Fe_3O_4 belongs to ion exchange adsorption and colloidal adsorption. In addition, the isothermal equation for adsorption of ATP/Fe_3O_4 generally conforms to the Freundlich and Langmuir equations [20,25]. Therefore, it is supposed that the ATP/Fe_3O_4 is probably fitted to the isotherms of Langmuir or Freundlich because of no hint of chemisorption occurrence for the system.

Future work for this project will involve development of Langmuir and Freundlich isotherms. However, when it comes to a complex mixture such as that of crude oil, using either the Langmuir or Freundlich isotherms is challenging [53]. This is due to the fact that not all components of crude oil obey these isotherms as single solutes, hence in order to calculate the constants for each isotherm one would need to be able to calculate the adsorption coefficient of each solute prior to the isotherm application [35].

4. Conclusions

Magnetic ATP was successfully prepared by the co-precipitation method, which exhibits a saturation magnetization of 1.5 emu/g, coercivity of 10 Oe, and residual magnetization of 0.03 emu/g. The magnetization of ATP is favorable for improving the thermal stability and dispersibility in the emulsified oil-water mixture. The magnetic ATP is easy and convenient to be recovered through an external magnetic field so as to save the operation cost and time. The adsorption capacity to emulsified oil slightly decreases from 8.14 to 7.16 mg/g even though the ATP is decorated with high loading Fe_3O_4. To further understand the adsorption mechanism, future work needs to involve the study of adsorption isotherms and adsorption kinetics. As such, it provides an important basis for realistic large-scale application. In summary, it is confident that the present work would lay a foundation for promising applications of functionalized ATP adsorbents for oily wastewater treatment.

Acknowledgements

We are grateful for the financial support of the Liaoning Natural Science Foundation of China (No. 2021-MS-238), the Liaoning BaiQianWan Talents Program (No. 2018921046), the Scientific Research Project of Liaoning Provincial Department of Education (No. LJGD2020002), and the Shenyang Youth Science and Technology Project (No. RC200325).

Conflict of interest

The authors declare no conflict of interest.

References

[1] H.J. Tanudjaja, C.A. Hejase, V.V. Tarabara, A.G. Fane, J.W. Chew, Membrane-based separation for oily wastewater: a practical perspective, Water Res., 156 (2019) 347–365.
[2] S. Kalla, Use of membrane distillation for oily wastewater treatment – a review, J. Environ. Chem. Eng., 9 (2021) 104641, doi: 10.1016/j.jece.2020.104641.
[3] C. Zhao, J. Zhou, Y. Yan, L. Yang, G. Xing, H. Li, P. Wu, M. Wang, H. Zheng, Application of coagulation/flocculation in oily wastewater treatment: a review, Sci. Total Environ., 765 (2021) 142795, doi: 10.1016/j.scitotenv.2020.142795.
[4] Z. Chen, Z. Zheng, C. He, J. Liu, R. Zhang, Q. Chen, Oily sludge treatment in subcritical and supercritical water: a review, J. Hazard. Mater., 433 (2022) 128761, doi: 10.1016/j.jhazmat.2022.128761.
[5] M. Wu, S. Song, T. Wang, W. Sun, S. Xu, Y. Yang, Natural sphalerite photocatalyst for treatment of oily wastewater produced by solvent extraction from spent lithium-ion battery recycling, Appl. Catal., B, 313 (2022) 121460, doi: 10.1016/j.apcatb.2022.121460.
[6] A. Ullah, H.J. Tanudjaja, M. Ouda, S.W. Hasan, J.W. Chew, Membrane fouling mitigation techniques for oily wastewater: a short review, J. Water Process. Eng., 43 (2021) 102293, doi: 10.1016/j.jwpe.2021.102293.
[7] W. Zheng, J. Huang, S. Li, M. Ge, L. Teng, Z. Chen, Y. Lai, Advanced materials with special wettability toward intelligent oily wastewater remediation, ACS Appl. Mater. Interfaces, 13 (2021) 67–87.
[8] Y. Su, Z. Li, H. Zhou, S. Kang, Y. Zhang, C. Yu, G. Wang, Ni/carbon aerogels derived from water induced self-assembly of Ni-MOF for adsorption and catalytic conversion of oily wastewater, Chem. Eng. J., 402 (2020) 126205, doi: 10.1016/j.cej.2020.126205.
[9] Y. Wang, Y. Li, J. Li, Y. Zhang, Z. Duan, F. Zhou, X. Xie, Q. Su, S. Pang, Attapulgite as a skeleton for the fabrication of magnetic structural-functional materials with a superhydrophobic shell, New J. Chem., 45 (2021) 10466–10480.
[10] R. Jiang, Z. Zhang, H. Chen, Y. Yu, Preparation of one-dimensional magnetic nanocomposites with palygorskites

as temples after inorganic modification, Colloids Surf., A, 619 (2021) 126520, doi: 10.1016/j.colsurfa.2021.126520.
[11] L. Zhang, F. Cao, J. Sun, Y. Sun, The synergistic effect of attapulgite in the highly enhanced photoreduction of Cr(VI) by oxalic acid in aqueous solution, Environ. Res., 197 (2021) 111070, doi: 10.1016/j.envres.2021.111070.
[12] P. Sun, W. Zhang, B. Zou, L. Zhou, Z. Ye, Q. Zhao, Preparation of EDTA-modified magnetic attapulgite chitosan gel bead adsorbent for the removal of Cu(II), Pb(II), and Ni(II), Int. J. Biol. Macromol., 182 (2021) 1138–1149.
[13] K.-Q. He, C.-G. Yuan, Y.-H. Jiang, Y. Li, X.-L. Duan, Q. Guo, Highly efficient sorption and immobilization of gaseous arsenic from flue gas on MnO_2/attapulgite composite with low secondary leaching risks, J. Cleaner Prod., 292 (2021) 126003, doi: 10.1016/j.jclepro.2021.126003.
[14] S.K. Bhagat, K. Pyrgaki, S.Q. Salih, T. Tiyasha, U. Beyaztas, S. Shahid, Z.M. Yaseen, Prediction of copper ions adsorption by attapulgite adsorbent using tuned-artificial intelligence model, Chemosphere, 276 (2021) 130162, doi: 10.1016/j.chemosphere.2021.130162.
[15] J. Liu, J. Zhang, L. Xing, D. Wang, L. Wang, H. Xiao, J. Ke, Magnetic Fe_3O_4/attapulgite hybrids for Cd(II) adsorption: performance, mechanism and recovery, J. Hazard. Mater., 412 (2021) 125237, doi: 10.1016/j.jhazmat.2021.125237.
[16] Y. Wang, Y. Feng, J. Jiang, J. Yao, Designing of recyclable attapulgite for wastewater treatments: a review, ACS Sustainable Chem. Eng., 7 (2019) 1855–1869.
[17] R.J. Zadeh, M.H. Sayadi, M.R. Rezaei, Synthesis of Thiol modified magMCM-41 nanoparticles with rice husk ash as a robust, high effective, and recycling magnetic sorbent for the removal of herbicides, J. Environ. Chem. Eng., 9 (2021) 104804, doi: 10.1016/j.jece.2020.104804.
[18] M. Khalatbary, M.H. Sayadi, M. Hajiani, M. Nowrouzi, Adsorption studies on the removal of malachite green by γ-Fe_2O_3/MWCNTs/cellulose as an eco-friendly nanoadsorbent, Biomass Convers. Biorefin., (2022), doi: 10.1007/s13399-022-02475-4.
[19] Y. Teng, Z. Liu, K. Yao, W. Song, Y. Sun, H. Wang, Y. Xu, Preparation of attapulgite/$CoFe_2O_4$ magnetic composites for efficient adsorption of tannic acid from aqueous solution, Int. J. Environ. Res. Public Health, 16 (2019) 2187, doi: 10.3390/ijerph16122187.
[20] Y. Wang, R. Zhou, C. Wang, G. Zhou, C. Hua, Y. Cao, Z. Song, Novel environmental-friendly nano-composite magnetic attapulgite functionalized by chitosan and EDTA for cadmium(II) removal, J. Alloys Compd., 817 (2020) 153286, doi: 10.1016/j.jallcom.2019.153286.
[21] R.Y. Hong, T.T. Pan, Y.P. Han, H.Z. Li, J. Ding, S. Han, Magnetic field synthesis of Fe_3O_4 nanoparticles used as a precursor of ferrofluids, J. Magn. Magn. Mater., 310 (2007) 37–47.
[22] Y. Liu, P. Liu, Z. Su, F. Li, F. Wen, Attapulgite–Fe_3O_4 magnetic nanoparticles via co-precipitation technique, Appl. Surf. Sci., 255 (2008) 2020–2025.
[23] Y. Deng, Y. Li, W. Nie, X. Gao, L. Zhang, P. Yang, X. Tan, Fast removal of propranolol from water by attapulgite/graphene oxide magnetic ternary composites, Materials, 12 (2019) 924, doi: 10.3390/ma12060924.
[24] M. Niu, Z. Li, W. He, W. Zhou, R. Lu, J. Li, H. Gao, S. Zhang, C. Pan, Attapulgite modified magnetic metal-organic frameworks for magnetic solid phase extraction and determinations of benzoylurea insecticides in tea infusions, Food Chem., 317 (2020) 126425, doi: 10.1016/j.foodchem.2020.126425.
[25] J. Ji, W. Xie, Removal of aflatoxin B1 from contaminated peanut oils using magnetic attapulgite, Food Chem., 339 (2021) 128072, doi: 10.1016/j.foodchem.2020.128072.
[26] S. Han, H. Yu, T. Yang, S. Wang, X. Wang, Magnetic activated-ATP@Fe_3O_4 nanocomposite as an efficient Fenton-like heterogeneous catalyst for degradation of ethidium bromide, Sci. Rep., 7 (2017) 6070, doi: 10.1038/s41598-017-06398-3.
[27] X. Zhang, B. Zhang, Y. Wu, T. Wang, J. Qiu, Preparation and characterization of a diatomite hybrid microfiltration carbon membrane for oily wastewater treatment, J. Taiwan Inst. Chem. Eng., 89 (2018) 39–48.
[28] L. Xu, Y. Liu, J. Wang, Y. Tang, Z. Zhang, Selective adsorption of Pb^{2+} and Cu^{2+} on amino-modified attapulgite: kinetic, thermal dynamic and DFT studies, J. Hazard. Mater., 404 (2021) 124140, doi: 10.1016/j.jhazmat.2020.124140.
[29] Y. Deng, Y. Li, Surface-bound humic acid increased propranolol sorption on Fe_3O_4/attapulgite magnetic nanoparticles, Nanomaterials, 10 (2020) 205, doi: 10.3390/nano10020205.
[30] F. Wang, B. Zhang, S. Liu, Y. Wu, T. Wang, J. Qiu, Investigation of the attapulgite hybrid carbon molecular sieving membranes for permanent gas separation, Chem. Eng. Res. Des., 151 (2019) 146–156.
[31] H. Wang, X. Wang, J. Ma, P. Xia, J. Zhao, Removal of cadmium(II) from aqueous solution: a comparative study of raw attapulgite clay and a reusable waste–struvite/attapulgite obtained from nutrient-rich wastewater, J. Hazard. Mater., 329 (2017) 66–76.
[32] H. Boleydei, N. Mirghaffari, O. Farhadian, Comparative study on adsorption of crude oil and spent engine oil from seawater and freshwater using algal biomass, Environ. Sci. Pollut. Res., 25 (2018) 21024–21035.
[33] F. Li, G. Miao, Z. Gao, T. Xu, X. Zhu, X. Miao, Y. Song, G. Ren, X. Li, A versatile hydrogel platform for oil/water separation, dye adsorption, and wastewater purification, Cellulose, 29 (2022) 4427–4438.
[34] D.N.H. Tran, S. Kabiri, T.R. Sim, D. Losic, Selective adsorption of oil-water mixtures using polydimethylsiloxane (PDMS)–graphene sponges, Environ. Sci. Water Res. Technol., 1 (2015) 298–305.
[35] F.A. Hussain, J. Zamora, I.M. Ferrer, M. Kinyua, J.M. Velázquez, Adsorption of crude oil from crude oil-water emulsion by mesoporous hafnium oxide ceramics, Environ. Sci. Water Res. Technol., 6 (2020) 2035–2042.
[36] H. Singh, A. Jain, J. Kaur, S.K. Arya, M. Khatri, Adsorptive removal of oil from water using SPIONs–chitosan nanocomposite: kinetics and process optimization, Appl. Nanosci., 10 (2020) 1281–1295.
[37] K. Okiel, M. El-Sayed, M.Y. El-Kady, Treatment of oil-water emulsions by adsorption onto activated carbon, bentonite and deposited carbon, Egypt. J. Pet., 20 (2011) 9–15.
[38] Y. Zhao, K. Zhong, W. Liu, S. Cui, Y. Zhong, S. Jiang, Preparation and oil adsorption properties of hydrophobic microcrystalline cellulose aerogel, Cellulose, 27 (2020) 7663–7675.
[39] H. Wang, C. Wang, S. Liu, L. Chen, S. Yang, Superhydrophobic and superoleophilic graphene aerogel for adsorption of oil pollutants from water, RSC Adv., 9 (2019) 8569–8574.
[40] J. Huang, Z. Yan, Adsorption mechanism of oil by resilient graphene aerogels from oil-water emulsion, Langmuir, 34 (2018) 1890–1898.
[41] R. Jazini Zadeh, M. Sayadi, M.R. Rezaei, Removal of 2,4-dichlorophenoxyacetic acid from aqueous solutions by modified magnetic nanoparticles with amino functional groups, J. Water Environ. Nanotechnol., 5 (2020) 147–156.
[42] R. Hosseini, M.H. Sayadi, H. Shekari, Adsorption of nickel and chromium from aqueous solutions using copper oxide nanoparticles: adsorption isotherms, kinetic modeling, and thermodynamic studies, Avicenna J. Environ. Health Eng., 6 (2019) 66–74.
[43] M.H. Sayadi, O. Rashki, E. Shahri, Application of modified *Spirulina platensis* and *Chlorella vulgaris* powder on the adsorption of heavy metals from aqueous solutions, J. Environ. Chem. Eng., 7 (2019) 103169, doi: 10.1016/j.jece.2019.103169.
[44] A. Farooghi, M.H. Sayadi, M.R. Rezaei, A. Allahresani, An efficient removal of lead from aqueous solutions using $FeNi_3$@SiO_2 magnetic nanocomposite, Surf. Interfaces, 10 (2018) 58–64.
[45] M.H. Sayadi, N. Salmani, A. Heidari, M.R. Rezaei, Bio-synthesis of palladium nanoparticle using *Spirulina platensis* alga extract and its application as adsorbent, Surf. Interfaces, 10 (2018) 136–143.
[46] A.L. Ahmad, S. Sumathi, B.H. Hameed, Adsorption of residue oil from palm oil mill effluent using powder and flake chitosan: equilibrium and kinetic studies, Water Res., 39 (2005) 2483–2494.

[47] H. Albatrni, H. Qiblawey, F. Almomani, S. Adham, M. Khraisheh, Polymeric adsorbents for oil removal from water, Chemosphere, 233 (2019) 809–817.
[48] S. Abbasi, M. Hasanpour, M.-S. Ekrami-Kakhki, Removal efficiency optimization of organic pollutant (methylene blue) with modified multi-walled carbon nanotubes using design of experiments (DOE), J. Mater. Sci.: Mater. Electron., 28 (2017) 9900–9910.
[49] S. Abbasi, M. Hasanpour, F. Ahmadpoor, M. Sillanpää, D. Dastan, A. Achour, Application of the statistical analysis methodology for photodegradation of methyl orange using a new nanocomposite containing modified TiO_2 semiconductor with SnO_2, Int. J. Environ. Anal. Chem., 101 (2021) 208–224.
[50] N. Ahmadpour, M.H. Sayadi, S. Sobhani, M. Hajiani, Photocatalytic degradation of model pharmaceutical pollutant by novel magnetic TiO_2@$ZnFe_2O_4$/Pd nanocomposite with enhanced photocatalytic activity and stability under solar light irradiation, J. Environ. Manage., 271 (2020) 110964, doi: 10.1016/j.jenvman.2020.110964.
[51] H. Shekari, M.H. Sayadi, M.R. Rezaei, A. Allahresani, Synthesis of nickel ferrite/titanium oxide magnetic nanocomposite and its use to remove hexavalent chromium from aqueous solutions, Surf. Interfaces, 8 (2017) 199–205.
[52] P. Karimi, S. Javanshir, M.H. Sayadi, H. Arabyarmohammadi, Arsenic removal from mining effluents using plant-mediated, green-synthesized iron nanoparticles, Processes, 7 (2019) 759, doi: 10.3390/pr7100759.
[53] R. Wahi, L.A. Chuah, T.S.Y. Choong, Z. Ngaini, M.M. Nourouzi, Oil removal from aqueous state by natural fibrous sorbent: an overview, Sep. Purif. Technol., 113 (2013) 51–63.